(E)ESI determination from mode-field diameter and refractive index profile measurements on single-mode fibres

F. Martinez, MSc
C.D. Hussey, PhD

Indexing terms: Measurements and measuring, Optical fibres, Waveguides and waveguide components

Abstract: We show, both experimentally and theoretically, that for single-mode fibres, the (E)ESI and MFD methods are interrelated in a self-consistent model with the theoretical cutoff wavelength playing a pivotal role. Three independent measurement approaches are examined: mode-field diameter measurements, preform profile measurements and fibre profile measurements.

1 Introduction

Currently, there are two trends in characterising single-mode fibres. They are:

(*a*) from refractive index profile measurements and

(*b*) from mode-field diameter (MFD) measurements.*

Between these two there exist equivalent step index (ESI) methods. The two ESI parameters (equivalent core-radius and equivalent numerical aperture) can be obtained from either the refractive index profile or the MFD. Having the ESI parameters and the MFD, we can predict most of the essential characteristics of single-mode fibres, such as bending loss, splice loss, microbending loss, waveguide dispersion (and therefore total dispersion). However, there is still confusion because there are several ESI definitions and measurement techniques, and several MFD definitions and measurement techniques, which have been proposed and none of them has been recognised as a standard method for characterising single-mode fibres.

In this paper, we propose a theory, which links the ESI parameters obtained from measurements of the refractive index profile to the same parameters derived from measurements of the MFD. We can therefore, in principle, unify both trends in characterising single-mode fibres. Measurements of refractive index profile and mode-field diameter are performed on MCVD fibres, to provide experimental support for this theory.

1.1 Equivalent step index (ESI) techniques

In general, the refractive index profile of a single-mode fibre deviates from the ideal step index as shown in Fig. 1. The problem is then to determine the propagation characteristics of a single-mode fibre with an arbitrary refractive index profile. Exact solutions are difficult to implement, and good approximate methods are preferred.

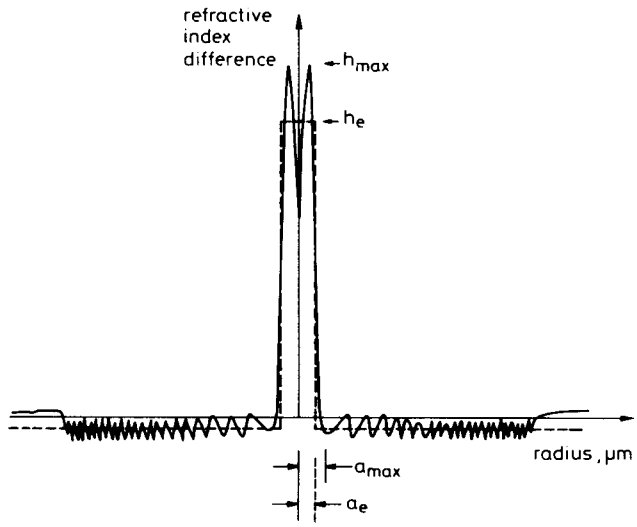

Fig. 1 *Typical refractive index profile of a MCVD single-mode fibre and a possible equivalent step index representation*

a_e is the equivalent core radius and h_e the equivalent index difference

——— actual refractive index profile

– – – – equivalent step-index profile

It has been observed that the fields of all single-mode fibres look similar. Since the analytical solutions for the step-index fibre are already available and well known, it is then very convenient to have a method which has as its reference a step-index fibre. This gives rise to equivalent step index methods.

The ESI fibre should have a second mode cutoff wavelength, fundamental mode propagation constant, MFD, and evanescent field as close as possible to the corresponding parameters of the actual fibre. If this is the case, the bending losses, microbending losses, and splice losses can be predicted from the ESI fibre [1].

There exist, however, some problems including [2]:

(*a*) Several ESI techniques are available, each of which gives different values for the two ESI parameters.

(*b*) The accuracy of the predicted propagation characteristics is not always good, particularly with the prediction of waveguide dispersion.

Referring to the latter problem, we have shown that one particular ESI method can be readily enhanced from the accurate prediction of waveguide dispersion [3], we

* Note: In addition to the term 'mode field diameter' MFD, we will use the term 'mode field radius' ω (i.e. MFD = 2ω). ω has also been referred as 'spot size' in the literature.

Paper 5954J (E13), received 19th October 1987

The authors are with the Optical Fibre Group, Department of Electronics and Computer Science, The University, Southampton, Hampshire SO9 5NH, United Kingdom

call this the enhanced ESI, or (E)ESI model. This model is based on the moments of the refractive index profile, and it proposes the use of an additional third parameter called the enhancement parameter. Unfortunately, performing refractive index profile measurements on the fibre is difficult and, occasionally, it is difficult to estimate the core diameter (i.e. core-cladding boundary) from the profile measurements. Because of these problems, the alternative of characterising single-mode fibres from MFD measurements has received a lot of attention.

1.2 Mode-field diameter measurement (MFD) techniques

The MFD is the width of the fundamental mode, guided by a single-mode fibre above its cutoff wavelength. MFD is in principle a very useful parameter, as it allows the prediction of splicing and microbending losses. In addition to that, the wavelength dependence of the MFD allows us to predict the bending losses (through the ESI parameters), and the waveguide dispersion.

However, quoting Reference 4, 'MFD appears to be a parameter in turmoil. Its importance is well understood, but no consensus on its fundamental definition or measurement method has yet emerged. Several measurement techniques and definitions have been proposed during the past few years. None of these methods is universally accepted as a reference test method, nor is any method more or less fundamentally correct than the others.'

The degree of consistency between the different techniques is a direct result of the choice of a definition for the MFD. The Gaussian approximation, as produced by Marcuse [5, 6] and illustrated in Fig. 2, so widely used

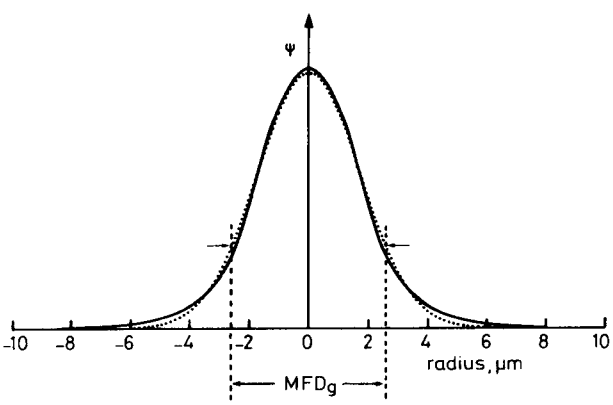

Fig. 2 *Field amplitude distribution of the fundamental mode, in a step-index single-mode fibre at V = 2.1, and its Gaussian approximation*

MFD_g is the Gaussian Mode-field diameter
——— actual field amplide distribution
····· gaussian approximation

for the first generation of single-mode fibres, is now severely questioned. Small systematic errors result even for quasistep index fibres when the Gaussian approximation is used, especially at longer wavelengths [7]. Also, the second generation, single-mode fibres with nonstep refractive indices for dispersion shifting and dispersion flattening do not exhibit Gaussian fields at any wavelength.

An alternative definition of MFD based, on the moments of the near-field, which is frequently called the Petermann 2 definition, can, in principle, solve the problem of consistency, and reduce the systematic errors [8]. The primary difference with respect to the Gaussian definition is that the Petermann definition uses the measured field directly, making no assumption about the shape of the field. Because of this, the Petermann 2 definition is becoming more widely accepted.

Cutoff wavelength is also essential in characterising single-mode fibres, but some problems arise because the second-mode becomes highly attenuated at wavelengths lower than the theoretical cutoff wavelength. This effective cutoff is dependent on the length and the bending of the fibre. There is some agreement on the effective cutoff definition and measurement techniques [9], but the relation between the effective and theoretical cutoff is presumably very difficult to determine. This suggests that one has to be careful when using the measured cutoff wavelength, as an input in the determination of the ESI parameters from the spectral variation of MFD, for example.

2 Unifying ESI and MFD methods in single-mode fibres

Millar's method is perhaps the most standard technique for determining the two ESI parameters and the second-mode cutoff wavelength for single-mode fibres. One basic assumption in the Millar method is that the MFD for arbitrary profiles behaves simply as a scaled version of the step-index MFD [10]. While this is true for most fibres used for telecommunications, it is not true in general, and in particular the method breaks down when applied to the triangular-type profile fibres and dual shape profile fibres [11] which are receiving a lot of attention for dispersion shifting.

In its simplest form, the Millar method measures the cutoff wavelength, together with the MFD. Unfortunately it is at the cutoff wavelength where the MFD is most sensitive (over the single-mode regime) to vagaries in the refractive index profile. Moreover, the Millar method has no built-in alarm to show that it breaks down for a specific fibre under measurement.

Here we show how the Millar method can be adapted to cater for a more complex MFD structure. Our approach uses the Petermann MFD [12, 13] (or far-field RMS width) to find the two parameters for the ESI or the three parameters necessary to specify the enhanced ESI (or (E)ESI). Having determined the three parameters, we can then decide whether to use all three parameters in the (E)ESI, or only two in the simple ESI approximation, but now we have a greater appreciation of the errors involved, if we choose the latter.

The implementation of our approach is aided by our analytic approximation to the Petermann MFD, which is outlined in Appendix 8.

2.2 Petermann MFD and (E)ESI approximation

The (E)ESI approximation is outlined in Appendix 8, and is specified by three parameters. For our purpose we will find it convenient to use the parameters $\bar{V}$, a_e, and $|\Delta\bar{\Omega}_4|$, where $\bar{V} = (2\pi/\lambda)a_e NA_e = \sqrt{(2\Omega_0)}V$, $a_e = a\sqrt{2\bar{\Omega}_2}$, and $NA_e = NA\sqrt{\Omega_0/\bar{\Omega}_2}$; a is the core radius, NA is the numerical aperture, Ω_0 is the guidance factor and Ω_n is the moment of profile. We can see from Appendix 7 that $\Delta\bar{\Omega}_4$ is the enhancement parameter; its magnitude gives an indication of the deviation of the refractive index from the step index (for which $\Delta\bar{\Omega}_4 = 0$). From Table 6, for example, we find that for the parabolic profile fibre, the enhancement parameter is 0.125, for the triangular profile fibre it is 0.190, and for cusp-like profiles, its value can approach 0.3.

In terms of our three parameters, the normalised near-field Petermann mode-field radius for fibres of arbitrary

profile can be expressed as [14]

$$\bar{\omega}^2 = \left(\frac{\omega}{a_e}\right)^2 = \left\{\frac{1}{\bar{\omega}_{st}^2(\bar{V})} + |\Delta\bar{\Omega}_4|\left[\frac{f(\bar{V})}{\bar{\omega}_{st}^2(\bar{V})} + \frac{\bar{V}^3 f'(\bar{V}) b_{st}(\bar{V})}{4}\right]\right\}^{-1} \quad (1)$$

where $b_{st}(\bar{V}) = (1.1428\bar{V} - 0.996)^2/\bar{V}^2$ is the Rudolph–Neumann approximation,

$$f(\bar{V}) = 0.0313 - 0.013\bar{V}^2 \quad (2)$$

(from Appendix 8.2), and

$$\bar{\omega}_{st} = 0.65 + 1.619\bar{V}^{-3/2} + 2.879\bar{V}^{-6} - (0.016 + 1.561\bar{V}^{-7}) \quad (3)$$

(from Appendix 8.1).

Since the first term in eqn. 1 represents the simple ESI, the full form of this equation illustrates dramatically the limitations of any procedure which arbitrarily attempts to fit a measured mode-field diameter with that of some step-index fibre. Additionally, the term in square brackets in eqn. 1 is a monotonically increasing function of V, so that by measuring the mode-field diameter at cutoff, we are choosing the worst sampling point for fitting the simple step-index mode field diameter for fibres which have a large enhancement parameter. These points are also illustrated in Fig. 3, where we plot $\bar{\omega}$ as a function of $\bar{V}$ for the triangular-profile fibre.

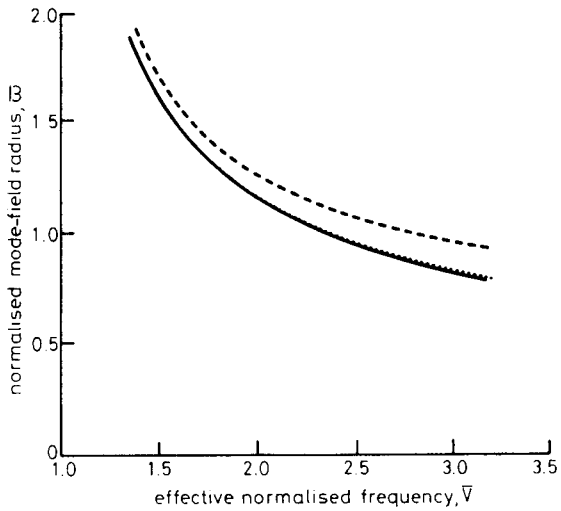

Fig. 3 *Mode-field radius $\bar{\omega}$ against $\bar{V}$ for the triangular profile fibre*
——— exact - - - ESI ····· enhanced ESI

It is convenient to rewrite eqn. 1 as follows:

$$\omega^2 = \frac{a_e^2}{p + |\Delta\bar{\Omega}_4| q} \quad (4)$$

where

$$p = \frac{1}{\bar{\omega}_{st}(V)}$$

$$q = f(\bar{V}) + \frac{\bar{V}^3 f'(\bar{V}) b_{st}(\bar{V})}{4}$$

The quantities p and q are specified once $\bar{V}$ is known. Similarly, the far-field mode radius can be expressed as

$$\omega_{ff}^2 = \frac{2}{\omega^2} = \frac{2}{a_e^2}(p + |\Delta\bar{\Omega}_4| q) \quad (5)$$

2.3 Adapted Millar procedure

The starting point of the Millar method [10] is the fact that the theoretical normalised cutoff frequency $\bar{V}_{co}$ is unlike any other fibre characteristic, because it is extremely insensitive to profile shape. The cutoff wavelength λ_{co} should therefore, in principle, be a fixed reference point for all single-mode fibre measurements.

Millar's method determines λ_{co} from observation of the near-field MFD behaviour. Further refinements have produced more accurate determinations of λ_{co} [15]. The possibility of using the far-field MFD behaviour in determining λ_{co} has also been suggested [16]. Such a technique could depend critically on the detector sensitivity.

By combining such a determination of the cutoff wavelength, with the measurement of the Petermann MFD at two different wavelengths (λ_1 and λ_2) in the single-mode region, i.e. $\lambda_1 \neq \lambda_2 \geqslant \lambda_{co}$, the three necessary parameters for specifying the (E)ESI are obtained as follows:

$$\bar{V}_{1,2} = 2.405\frac{\lambda_{co}}{\lambda_{1,2}} \quad (6a)$$

$$|\Delta\bar{\Omega}_4| = \frac{p_1 - Rp_2}{Rq_2 - q_1} \quad (6b)$$

$$a_e^2 = \omega_1^2(p_1 + |\Delta\bar{\Omega}_4| q_1) = \omega_2^2(p_2 + |\Delta\bar{\Omega}_4| q_2) \quad (6c)$$

where R is the ratio of the two mode field radius measurements, (ω_2^2/ω_1^2), $p_{1,2}$ and $q_{1,2}$ are the values of p and q of eqn. 2 evaluated at $\bar{V}_{1,2}$, and $\omega_{1,2}$ are the measured values of the near-field mode field radius at $\lambda_{1,2}$.

If we use the far-field RMS width measurements at the two different wavelengths, then the parameters $\bar{V}_{1,2}$ and $|\Delta\bar{\Omega}_4|$ are still given by eqns. 6*a* and *b*, while the equivalent core radius is now:

$$a_e = \frac{2}{\omega_{ff1}^2}(p_1 + |\Delta\bar{\Omega}_4| q_1) = \frac{2}{\omega_{ff2}^2}(p_2 + |\Delta\bar{\Omega}_4| q_2) \quad (6d)$$

while R in eqn. 6*b* is now defined as $(\omega_{ff1}^2/\omega_1^2)$.

The two-parameter ESI can be obtained from measurements of the Petermann MFD at one wavelength, together with the cutoff wavelength. Neglecting the enhancement parameter (i.e. $|\Delta\bar{\Omega}_4| = 0$ in eqn. 6*c*, then the two parameters are given by:

$$\bar{V}_i = 2.405\frac{\lambda_{co}}{\lambda_i} \quad (7)$$

and

$$a_e = \frac{\omega_i}{\bar{\omega}_{st}(\bar{V}_i)} \quad (8)$$

and $\bar{\omega}_{st}(\bar{V}_i)$ can be given by eqn. 3. The subscript i now corresponds to any wavelength about the cutoff wavelength.

The equivalent numerical aperture NA_e is now obtained simply from $NA_e = 2.405\lambda_{co}/2\pi a_e$.

3 Measurements

In this paper we implement and critically assess our approach using three independent measurement procedures. The (E)ESI parameters as obtained from MFD measurements, preform profile measurements, and fibre

profile measurements, are compared for a nominally step index fibre fabricated by the MCVD process.

A statistical approach is adopted in analysing the measurement data, thereby reducing the influence of measurement error and other inherent uncertainties. Results show that while the preform and the fibre profile measurements produce essentially the same equivalent core radius and the same equivalent numerical aperture (with allowance for diffusion effects), the ESI parameters produced by the MFD are substantially different.

The discrepancy arises from the use of the effective cutoff wavelength, as derived from the MFD measurements, instead of the theoretical cutoff wavelength (corresponding to a $\bar{V}$ value of 2.405) in the evaluation of the ESI parameters.

However, it is found that if the theoretical cutoff wavelength, as derived from the profile measurements, is used in the interpretation of the MFD data, then the three measurement approaches predict very similar ESI parameters. While only one fibre-preform is reported here, one other nominally step-index fibre-preform exhibited similar trends.

3.1 Profile measurements

Figs. 4*a* and 4*b* show the refractive index profiles of the preform and the fibre, respectively, as measured using commercial equipment (spatial filtering technique and refracted near-field technique, respectively). The (E)ESI parameters were derived from the moment analysis of the refractive index profile for the preform and the fibre. Problems in implementing this procedure arise because both the core radius and the refractive index levels of the core and the cladding are not well defined. Because of this, six limits were proposed, as sketched in the insets of Fig. 4. When using the preform data, the same measured core radii as used for points 1, 2, 3, 4, 5 and 6 in Fig. 4*b* were assigned for the corresponding points in Fig. 4*a*. Assuming circular symmetry only, the right hand half of each profile has been used.

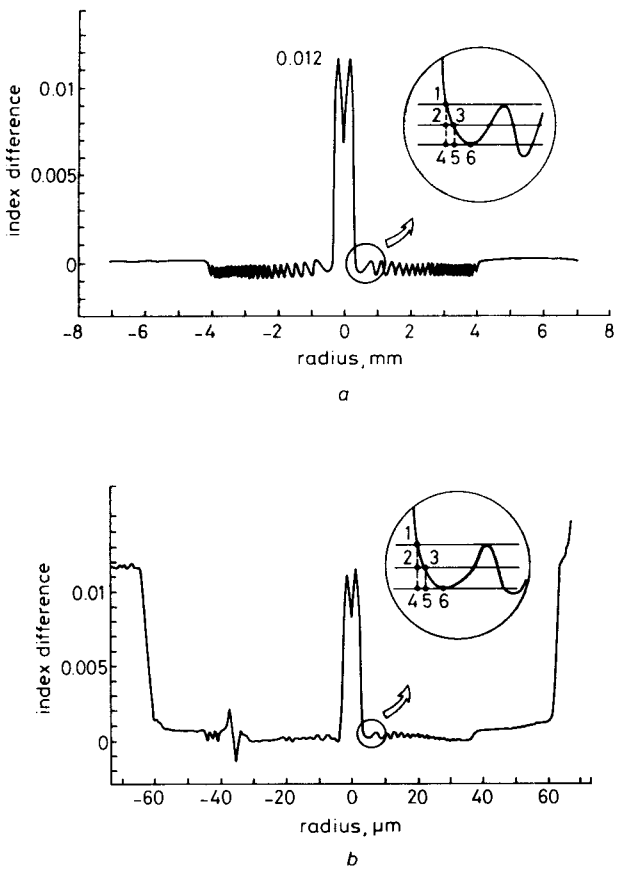

Fig. 4 *Refractive index profile of (a) preform and (b) fibre*
The insets show the six different core sizes and cladding levels used

The (E)ESI parameters resulting from the profile measurements also differ slightly from one choice of profile to another. Table 1 shows the average (E)ESI parameters resulting from the six profiles, both for the fibre and the preform.

Table 1: Average (E)ESI parameters as obtained from refractive index profile measurements and moments theory

Parameter	Profile measurements	
	Fibre	Preform
λ_{co}(nm)	1226 ± 25	1217 ± 11
a_e(μm)	2.86 ± 0.12	2.71 ± 0.1
NA_e	0.164 ± 0.005	0.1722 ± 0.0007
$\lvert\Delta\tilde{\Omega}_4\rvert$	0.08 ± 0.02	0.03 ± 0.01

(Average theoretical cutoff is $\lambda_{co} = 1222$ nm). The uncertainty quoted is the standard deviation

3.2 Mode-field diameter measurements

The near-field Petermann's MFD was obtained from the inverse of the RMS far-field width measured by the variable aperture method using commercial equipment. The cutoff wavelength was measured using two techniques:

(*a*) the Millar procedure from the variation of MFD as a function of wavelength

(*b*) the transmitted power technique (as recommended by CCITT) [17].

Table 2 shows the values measured for the Petermann's MFD at four wavelengths. In theory, for the determination of the (E)ESI parameters, the cutoff wavelength together with the MFD at any other two wavelengths are sufficient. In practice, if we try different wavelength pairs we obtain different results. Our approach is to take the average value of the (E)ESI parameters predicted from different pairs of the four wavelengths in Table 2. Table 3 shows the average value of these (E)ESI parameters for the two different measured cutoff wavelengths.

Table 2: Near-field Petermann's MFD at four wavelengths for the fibre used in the comparative analysis

λ (nm)	Petermann's MFD (μm)
1300	6.47 ± 1%
1350	6.64 ± 1%
1400	6.85 ± 1%
1450	7.07 ± 1%

Table 3: Average (E)ESI parameters as obtained from MFD measurements

Parameter	λ_{co1} = 1275 ± 25 (nm)	λ_{co2} = 1295 ± 25 (nm)
a_e(μm)	3.16 ± 0.12	3.22 ± 0.14
NA_e	0.155 ± 0.006	0.154 ± 0.007
$\lvert\Delta\tilde{\Omega}_4\rvert$	0.13 ± 0.08	0.14 ± 0.09

λ_{co1} was measured using the transmitted power technique. λ_{co2} was measured using the variation of MFD as a function of wavelength

If we choose to ignore the enhancement parameter in determining the two parameters of the simple ESI, we require the cutoff wavelength and the MFD at only one wavelength. We again determine the average values from

Table 4: Average (E)ESI parameters derived from MFD measurements assuming $|\Delta\bar{\Omega}_4| = 0$

Parameter	$\lambda_{co1} = 1275 + 25$ (nm)	$\lambda_{co2} = 1295 \pm 25$ (nm)
$a_e(\mu m)$	2.94 ± 0.005	2.97 ± 0.008
NA_e	0.1662 ± 0.0003	0.1668 ± 0.0004

λ_{co1} and λ_{co2} as in Table 3

the measurements in Table 1. These are shown in Table 4 for the two different measured cutoff wavelengths.

4 Discussion of results

Taking the results for the profile measurements in Table 1, it is found that the two parameters a_e and NA_e are in good agreement between the fibre and the preform. However, there is a slight increase in a_e and a slight decrease in NA_e in the transition from preform to fibre, this is consistent with the occurrence of diffusion during fibre drawing. The fact that there is only a slight variation in these parameters from preform to fibre is interesting, since these two parameters are derived from the first two even moments of the profile shape function, and as such they rely on the average properties of the refractive index profile which are not expected to change very much in the fibre draw. It should be pointed out that the poor resolution in the fibre profile measurement will also appear as diffusion, however, even within the error bound there is an overall true diffusion effect. In addition, the theoretical cutoff wavelengths, as derived from:

$$\lambda_{co} = 2\pi a_e NA_e/2.405 \tag{9}$$

are in good agreement between fibre and preform.

The enhancement parameter $|\Delta\bar{\Omega}_4|$ is small in both cases of preform and fibre profile measurements. The average value of the enhancement parameter of the preform is $|\Delta\bar{\Omega}_4| = 0.03$, and according to Table 6, it corresponds approximately to a power-law profile with $\alpha = 8$, which is very step-like. The enhancement parameter in the fibre ($|\Delta\bar{\Omega}_4| = 0.08$) again, according to Table 6, corresponds approximately to a power-law profile with $\alpha \approx 4$ which is also very step-like. The enhancement parameter is therefore small enough to be neglected, because its effect on the dispersion parameters b, b_1 and b_2 is small (see Appendix 8), and therefore its influence on the behaviour of the MFD is also very small. It is also interesting to note that $|\Delta\bar{\Omega}_4|$ in the fibre is slightly larger than in the preform. This gives a measurement of the slight diffusion that occurs in the profile of a single-mode fibre when it is drawn from the preform. The comparatively larger standard deviation in the determination of the (E)ESI parameters for the fibre is an indication of the intrinsic difficulty when working with the small dimensions involved.

Table 5: Average (E)ESI parameters as obtained from MFD measurements, but using now the average theoretical cutoff wavelength ($\lambda_{co} = 1222$ nm) derived from the refractive index profile and moments theory

Parameter	(E)ESI	ESI
$a_e(\mu m)$	3.0 ± 0.07	2.84 ± 0.01
NA_e	0.156 ± 0.003	0.1649 ± 0.0004
$\lvert\Delta\bar{\Omega}_4\rvert$	0.09 ± 0.05	—

Table 6: Data for the first two moments (Ω_0 and $\bar{\Omega}_2$) and for the enhancement parameter $\Delta\bar{\Omega}_4$ for several values of the exponent α of the power-law profiles

α	Ω_0	$\bar{\Omega}_2$	$\Delta\bar{\Omega}_4$
∞	0.500	0.500	0.000
16	0.444	0.450	0.010
8	0.400	0.417	0.029
4	0.333	0.375	0.067
2	0.250	0.333	0.125
1	0.167	0.300	0.190
$\frac{3}{4}$	0.136	0.289	0.215
$\frac{1}{2}$	0.100	0.278	0.246
$\frac{1}{4}$	0.056	0.265	0.285

On examining the results from the MFD measurements in Table 3, it is found that the results are completely at odds with those from the profiles. The discrepancy is due to the use of the measured cutoff wavelength (λ_{mco}) in determining the fibre parameters from eqn. 9. On substituting the average theoretical cutoff value λ_{co} deduced from the profiles (i.e. $\lambda_{co} =$ 1222 nm) into the MFD analysis, the parameter values as shown in Table 5 are obtained. These parameters are now in good agreement with those derived from the fibre profile.

From Table 5 we can conclude, as we have done for the profiles, that the simple two parameter ESI should be adequate for this fibre. Indeed the simple two parameter ESI results in this Table are found to be in remarkably good agreement with those in Table 1, once we use the theoretical cutoff wavelength in the analysis.

5 Conclusions

We show that the theoretical cutoff wavelength, as defined by eqn. 9, is the key to obtaining a self-consistent model for characterising single-mode fibres which unites both the ESI and MFD models. The measured cutoff wavelength, which for a given fibre remains consistent between different reference measurement techniques, does not have a definite relationship to the theoretical cutoff wavelength when comparing different fibres. As such, the measured cutoff wavelength can lead only to confusion when used as a reference wavelength in determining the ESI parameters. This conclusion is drawn not only from the results from a single fibre as presented here, but also from other experimental results in our laboratory, and from results quoted by other workers (such as in References 18 and 19).

One of the limitations of the MFD measurements presented here is the restricted set of data. Ideally, a larger number of measurements would improve the results for the average and the standard deviation of the (E)ESI parameters. This, however, would increase the time spent performing the measurements.

6 Acknowledgments

This work was supported by the SERC. The authors would like to thank Dr. N. McFarlane from York Technology for performing the mode-field diameter measurements. Mr. Martinez would also like to thank the Mexican Institutions CONACYT and IIE for their support.

7 References

1 JEUNHOMME, L.B.: 'Single-mode fibre optics: Principles and applications' (Marcel Dekkr. Ing, New York, 1983)
2 SAMSON, P.J.: 'Usage-based comparison of ESI techniques', *J. Lightwave Tech.*, 1985, **LT-3**, pp. 165–175
3 MARTINEZ, F., and HUSSEY, C.D.: 'Enhanced ESI for the prediction of waveguide dispersion in single-mode optical fibres', *Electron. Lett.*, 1984, **24**, pp. 1019–1021

4 DICK, J.M., and SHAAR, C.: 'Mode field diameter: toward a standard definition', *Laser and Appl.*, 1986, **5**, pp. 91–94
5 MARCUSE, D.: 'Loss analysis of single-mode fibre splices', *Bell Syst. Tech. J.*, 1977, **56**, pp. 703–718
6 MARCUSE, D.: 'Gaussian approximation for single-mode fibres', *J. Opt. Soc. Am.*, 1978, **68**, pp. 103–109
7 SARAVANOS, C., and LOWE, R.S.: 'The measurement of non-gaussian mode fields by the far-field axial scanning technique', *J. Lightwave Tech.*, 1986, **LT-4**, pp. 1563–1566
8 ANDERSON, W.T.: 'Status of single-mode fibre measurements'. Technical Digest Symposium on Optical Fibre Measurements, National Bureau of Standards, U.S. Department of Commerce, 1986, pp. 77–90
9 FRANZEN, O.C.: 'Determining the effective cutoff wavelength of single-mode fibres: An interlaboratory comparison', *J. Lightwave Tech.*, 1985, **LT-3**, pp. 128–134
10 MILLAR, C.: 'Direct method for determining equivalent step index profiles for monomode fibres', *Electron. Lett.*, 1981, **17**, pp. 458–460
11 OGAI, M., KINOSHITA, E., TAMURA, J., NAKAMURA, S., and HIGASHIMOTO, M.: 'Low-loss dispersion shifted fibre with dual shape refractive index profile', *Tech. Dig. ECOC '87*, **1**, pp. 171–174
12 PETERMANN, K.: 'Constraints for fundamental modal spot size for broadband dispersion compensated single-mode fibres', *Electron. Lett.*, 1984, **19**, pp. 712–714
13 HUSSEY, C.D.: 'Field to dispersion relationships in single-mode fibres', *ibid.*, 1984, **20**, pp. 1051–1052
14 HUSSEY, C.D., and MARTINEZ, F.: 'New interpretation of spot-size measurements on singly-clad single-mode fibres', *ibid.*, 1986, **22**, pp. 28–30
15 CAMPOS, A.C., SRIVASTAVA, R., and ROVERSI, J.A.: 'Characterization of single-mode fibres from wavelength dependence of modal field and far field', *J. Lightwave Tech.*, 1984, **LT-2**, pp. 334–340
16 PASK, C., and RUHL, F.: 'New method for equivalent-step index fibre determination', *Electron. Lett.*, 1983, **19**, pp. 658–659
17 CCITT: Recommendation G.652: 'Characterization of single-mode optical fibre cable', Section III: 'Test methods for the cutoff wavelength'
18 PASK, C., and RUHL, F.: 'Effects of loss on equivalent-step index fibre determination', *Electron. Lett.*, 1983, **19**, pp. 643–644
19 FOX, M.: 'Calculation of equivalent-step-index parameters for single-mode fibres', *Opt. and Quant. Electron.*, 1983, **15**, pp. 451–455
20 HUSSEY, C.D., and MARTINEZ, F.: 'Approximate analytical forms for the propagation characteristics of single-mode optical fibres', *Electron. Lett.*, 1985, **21**, pp. 1103–1104
21 RUDOLPH, H.D., and NEUMANN, E.G.: 'Approximation for the eigenvalues of the fundamental mode of a step index glass fibre waveguide', *Nachrichtentech. Z.*, 1976, **29**, pp. 328–329
22 HUSSEY, C.D., and PASK, C.: 'Theory of profile moments description of single-mode fibres', *IEE Proc. H.*, 1982, **129**, pp. 123–134
23 GAMBLING, W.A., MATSUMURA, H., and RAGDALE, C.M.: 'Mode dispersion, material dispersion and profile dispersion in graded index single-mode fibres', *Microwave, Optics and Acoustics*, 1979, **3**, pp. 239–245

8 Appendix

8.1 *Approximate analytical forms for the propagation characteristics of the single-mode fibres*

We present an approximate analytic form for the Petermann mode field radius, as required in the paper. The new equation adds two extra terms to the old Marcuse mode field radius expression [7].

8.1.1 Mode field radius and eigenvalue: The exact analytical formula for the normalised Petermann 2 mode field radius, $\bar{\omega}_p$, $(\sqrt{2}/W)(J_1(U)/J_0(U))$ can be expressed approximately as [20]:

$$\bar{\omega}_p = \bar{\omega}_M - (0.016 + 1.561V^{-7}) \tag{10}$$

where $\bar{\omega}_M$ is the Marcuse formula for the normalised mode field radius of an optimally exciting Gaussian beam, and which we repeat here for convenience [5]:

$$\bar{\omega}_M = 0.650 + 1.619V^{-3/2} + 2.879V^{-6} \tag{11}$$

For our purposes we have optimised eqn. 10 to be accurate to within 1% in the region $1.5 \leqslant V \leqslant 2.5$, since this is the range of most practical interest in single-mode fibre transmission. Like the Marcuse formula, eqn. 10 was determined empirically. Increased accuracy over a more extended range would require additional terms, and would be of questionable advantage.

Fig. 5 shows $\bar{\omega}_M$, and both the exact and approximate curves for $\bar{\omega}_p$. The very good accuracy of eqn. 10 for larger V values ($V > 2.5$), and the good qualitative

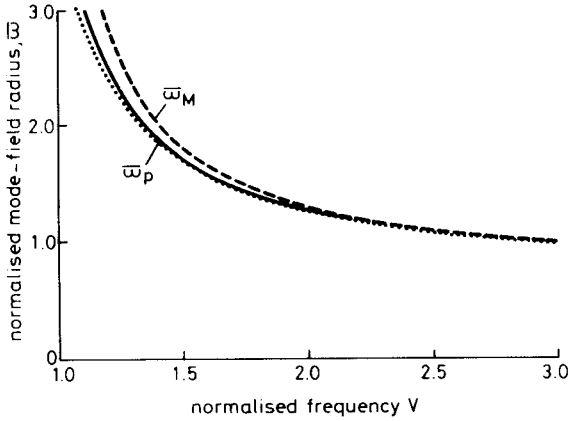

Fig. 5 *Petermann mode-field radius $\bar{\omega}_p$ and Marcuse mode-field radius $\bar{\omega}_M$ plotted as a function of normalised frequency V*
Petermann (exact)
Petermann (approximate)
Marcuse

behaviour for small V values ($V < 1.5$) are additional bonuses.

For completeness and easy reference we also include here the Rudolph–Neumann approximation for the modal eigenvalue, which is given by (see reference 21):

$$W = 1.1428V - 0.996 \quad 1.5 \leqslant V \leqslant 2.5 \tag{12}$$

This is accurate to within 0.1% for our chosen range.

8.1.2 Other propagation characteristics: The dispersion parameters b, b_1, and b_2 and the fraction of power propagation in the core, η, have been shown to be intimately related to the normalized Petermann mode field radius $\bar{\omega}_p$ [13], namely

$$b_2 = 4\frac{d}{dV}\left(\frac{1}{V^2\bar{\omega}_p^2}\right) \tag{13a}$$

$$b_1 = \frac{4}{V^2\bar{\omega}_p^2} + b \tag{13b}$$

$$\eta = \frac{2}{V^2\bar{\omega}_p^2} + b \tag{13c}$$

We propose to use eqns. 10 and 12 in eqns. (13*a–c*), thereby eliminating the need for numerical methods in evaluating eigenvalue or Bessel function terms.

The accuracy of this approach is illustrated in Fig. 6 for our parameters b, b_1, b_2, and η. The curve for b is simply the well-known Rudolph–Neumann approximation. The curves for b_1 and η are of remarkable accuracy: they are within 1% for our chosen range, and do not deteriorate appreciably beyond this range. For low V values, we are clearly obtaining a compensating effect of a poor eigenvalue combined with a poor mode field radius to give good results. The parameter b_2 has always been the severest test of any approximation, since it relies on derivatives for its determination. In this case, however, the result is clearly impressive; the accuracy at $V = 1.5$ is 1.6%, and is well within this over the most of the range

(1.5 ≤ V ≤ 2.5). The percentage accuracy at large V values becomes meaningless, since the function is approaching zero; however, a good indication of its validity is that the approximation predicts the zero dispersion point ($V_{zd} \approx 3$) to within 2%.

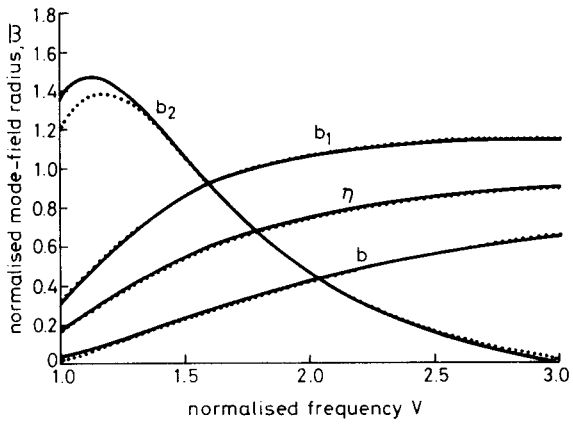

Fig. 6 *Approximate and exact dispersion and core power curves plotted as functions of normalised frequency V*

—— exact ····· approximate

8.2 ESI and (E)ESI based on the moments of the refractive index profile

The model we use is based on the moments of the refractive index shape function, and is much easier to use than a similar model proposed in Reference 22.

8.2.1 Moments definition: The profile moments are defined as

$$\Omega_M = \int_0^1 s(R) R^{M+1}\, dR \tag{14}$$

where $s(R)$ is the profile shape function

$$s(R) = \frac{n^2(r) - n_{cl}^2}{n_0^2 - n_{cl}^2} \tag{15}$$

which can be rewritten as

$$s(R) \approx \frac{n(r) - n_{cl}}{n_0 - n_{cl}} \tag{16}$$

Since the fibres are weakly guiding, $R = r/\rho$ (r is the usual radial variable), ρ is the core radius, $n(r)$ is the refractive index distribution, n_0 and n_{cl} are the maximum core and uniform cladding refractive indices, respectively.

The shape function $s(R)$ has a maximum of 1, i.e. $0 \leq s(R) \leq 1$, in the region $0 < R < 1$ and $s(R) = 0$ for $R > 1$.

The normalised moments are defined by

$$\bar{\Omega}_M = \frac{\Omega_M}{\Omega_0} \tag{17}$$

and it has been established that only the even moments ($\Omega_0, \Omega_2, \Omega_4, \ldots$) are required to specify any refractive index distribution [22].

The ESI requires that the first two even moments (Ω_0, $\bar{\Omega}_2$) of both the actual profile and the equivalent step profile are equal. This condition renders an equivalent step with a core radius of:

$$\rho_e = \sqrt{(2\bar{\Omega}_2)} \tag{18a}$$

and a profile height of:

$$h_e = \frac{\Omega_0}{\bar{\Omega}_2} \tag{18b}$$

The average waveguide parameter, $\bar{V}$, is related to the usual waveguide parameter V by

$$\bar{V} = \sqrt{(2\Omega_0)} V \tag{19}$$

Using the average waveguide parameter and the ESI, defined by eqn. 18, the dispersion expressions take the following forms:

$$b(V) = \frac{W^2}{V^2} \approx \left(\frac{\Omega_0}{\bar{\Omega}_2}\right) b_{st}(\bar{V}) \tag{20a}$$

$$b_1(V) = \frac{d(Vb)}{dV} \approx \left(\frac{\Omega_0}{\bar{\Omega}_2}\right) b_{1st}(\bar{V}) \tag{20b}$$

$$b_2(V) = \frac{V d(b_1)}{dV} \approx \left(\frac{\Omega_0}{\bar{\Omega}_2}\right) b_{2st}(\bar{V}) \tag{20c}$$

where $b_{st}(\bar{V})$ is evaluated for the step index fibre at $V = \bar{V}$.

Any error introduced in using this ESI, is caused by neglecting the difference between the higher moments of the profile $\bar{\Omega}_M$ and the higher moments of ESI, Ω_{Mst}. We define the normalised difference as follows:

$$\Delta\bar{\Omega}_M = \frac{(\bar{\Omega}_M - \bar{\Omega}_{Mst})}{\bar{\Omega}_{Mst}} \tag{21}$$

where $M \geq 4$.

M is even and

$$\bar{\Omega}_{Mst} = \frac{(2\bar{\Omega}_2)^{M/2}}{M/2 + 1} \tag{22}$$

In enhancing the simple ESI model, we introduce the effects of adding only one extra parameter, this is the enhancement parameter $\Delta\bar{\Omega}_4$.

Using eqns. 21 and 22, $\Delta\bar{\Omega}_4$ can be expressed more specifically as:

$$\Delta\bar{\Omega}_4 = \frac{(3/4)\bar{\Omega}_4 - \bar{\Omega}_2^2}{\bar{\Omega}_2^2} \tag{23}$$

We have, therefore adopted the following functional form for the dispersion parameter $b(V)$:

$$b(V) = \left(\frac{\Omega_0}{\bar{\Omega}_2}\right) b_{st}(\bar{V})[1 + |\Delta\bar{\Omega}_4| f(\bar{V})] \tag{24}$$

This is an enhancement of the simpler expression of eqn. 20*a* where $f(\bar{V})$ is our enhancement function. We will refer to eqn. 24 as the Enhanced ESI, or (E)ESI approximation for $b(V)$.

Table 6 shows $\Delta\bar{\Omega}_4$ for several α values of the power law profiles. $\Delta\Omega_4$ decreases as we approach the step-index fibre; the correction term in eqn. 24 decreases accordingly. The size of $\Delta\bar{\Omega}_4$ can be used to decide whether or not the function $f(\bar{V})$ is required.

8.2.2 The (E)ESI and its prediction of dispersion: From the exact calculation of $b(V)$ for a range of profiles, we found the lowest-order polynomial approximated for $f(\bar{V})$ to be the quadratic

$$f(\bar{V}) = 0.313\bar{V} - 0.013\bar{V}^2 \tag{25}$$

The power law profiles with exponent α have been used for testing the (E)ESI model, and the main results are described as follows:

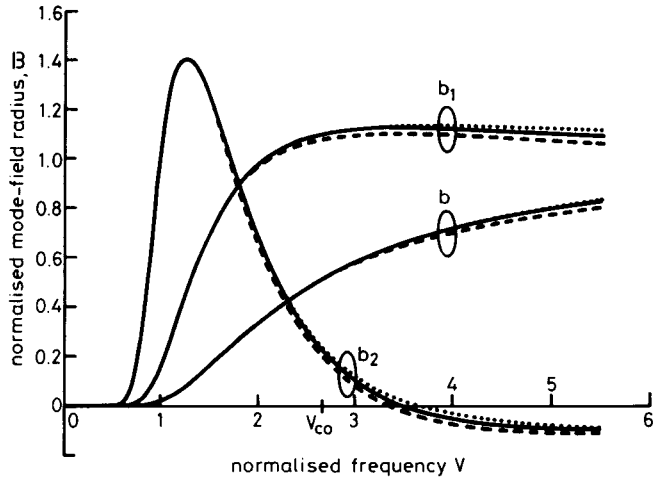

Fig. 7 *Comparison between the dispersion curves b, b_1, and b_2 obtained by using:*

a An exact numerical technique
b The Enhanced ESI
c The simple ESI approximation
The results are for the power-law profile with $\alpha = 8$. V_{co} indicates the limit of single-mode operation
—— exact ····· EESI - - - - ESI

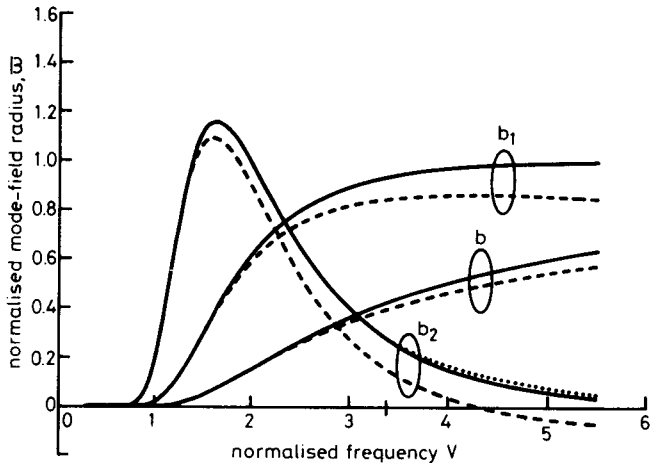

Fig. 8 *As Fig. 7, with* $\alpha = 2$
—— exact ····· EESI - - - - ESI

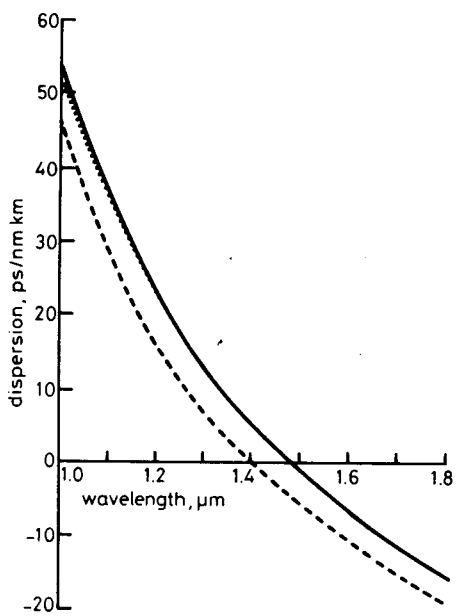

Fig. 9 *Total dispersion for the parabolic index profile fibre* ($\alpha = 2$)
—— exact ····· EESI - - - - ESI

(*a*) Profiles with $\alpha \geqslant 2$. For profiles which range from the clad parabola ($\alpha = 2$) to the step index ($\alpha = \infty$), the error in predicting the dispersion parameters is negligible in the single-mode region. Figs. 7 and 8 show the exact ESI and (E)ESI dispersion curves for $\alpha = 8$ and $\alpha = 2$, respectively.

Fig. 9 shows the ESI, (E)ESI and exact total dispersion curves for the clad parabolic core profile ($\alpha = 2$). The curves were obtained using the equation of the components of total dispersion, and data of Reference 23, and the ESI and (E)ESI dispersion parameters b, b_1, and b_2. It is seen that the total dispersion curve predicted by the EESI and the exact curve are, for all practical purposes, the same. The wavelength of zero total dispersion (λ_{OTD}) is predicted exactly by the (E)ESI, while the λ_{OTD} is in error by 5.4% for the simple ESI.

(*b*) Profiles with $\alpha < 2$. For these extreme profiles it has been found that the (E)ESI provides the bulk of the correction term for waveguide dispersion in the range of V-values for which the simple ESI breaks down. Fig. 10

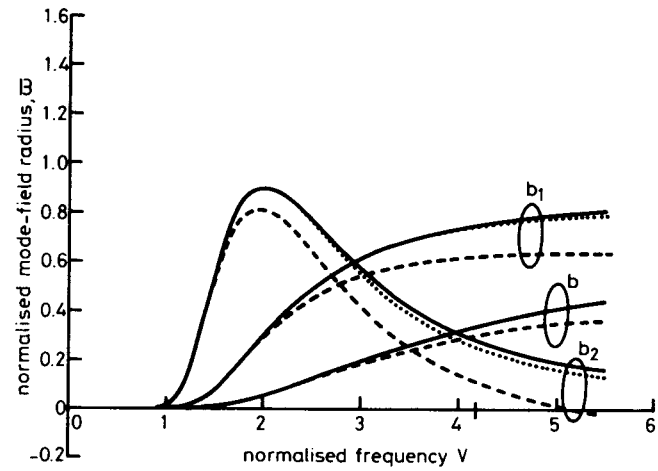

Fig. 10 *As Fig. 7 with* $\alpha = 1$
—— exact ····· EESI - - - - ESI

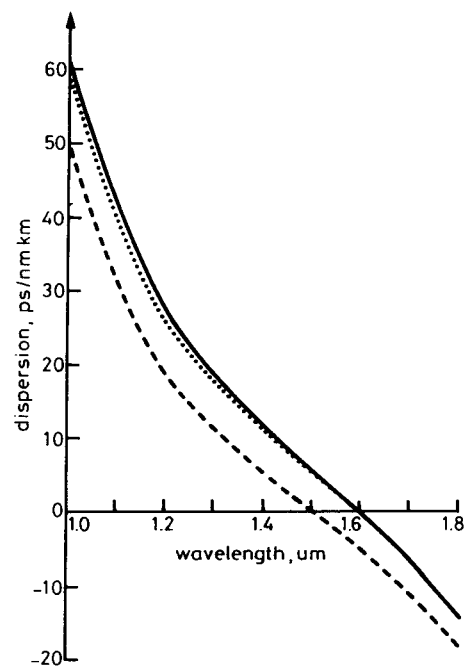

Fig. 11 *Total dispersion for the triangular index profile fibre* ($\alpha = 1$)
—— exact ····· EESI - - - - ESI

illustrates the triangular profile ($\alpha = 1$) case. For the triangular profile, the (E)ESI provides an estimate of the waveguide dispersion paramater, $b_2(V)$, of 92% of its exact value at the cutoff of the second mode, and improves rapidly for smaller V-values. In this case, the estimate of b and b_1 are accurate.

Fig. 11 shows the ESI, (E)ESI, and exact total dispersion curves for the triangular core profile fibre. The (E)ESI total dispersion curve is in good agreement with the exact calculation, and λ_{0TD} is the same for both the exact and (E)ESI curves. The ESI approximation predicts the zero of total dispersion with an error of 6.7%.